Limiting ionic conductivity and solvation dynamics in formamide

Hemant K. Kashyap, Tuhin Pradhan, and Ranjit Biswas[a)]
S. N. Bose National Centre for Basic Sciences, JD Block, Sector III, Salt Lake, Kolkata 700 098, India

(Received 13 June 2006; accepted 10 October 2006; published online 7 November 2006)

A self-consistent microscopic theory has been used to calculate the limiting ionic conductivity of unipositive rigid ions in formamide at different temperatures. The calculated results are found to be in good agreement with the experimental data. The above theory can also predict successfully the experimentally observed temperature dependence of total ionic conductivity of a given uniunivalent electrolyte in formamide. The effects of dynamic polar solvent response on ionic conductivity have been investigated by studying the time dependent progress of solvation of a polarity probe dissolved in formamide. The intermolecular vibration (libration) band that is often detected in the range of 100–200 cm^{-1} in formamide is found to play an important role in determining both the conductivity and the ultrafast polar solvent response in formamide. The time dependent decay of polar solvation energy in formamide has been studied at three different temperatures, namely, at 283.15, 298.15, and 328.15 K. While the predicted decay at 298.15 K is in good agreement with the available experimental data, the calculated results at the other two temperatures should be tested against experiments. © *2006 American Institute of Physics*. [DOI: 10.1063/1.2387947]

I. INTRODUCTION

Formamide and its substituted derivatives constitute an important class of solvent.[1–12] These liquids are characterized by large values of permanent dipole moments and dielectric constants. These solvents are also strong hydrogen bond (H-bond) donors and are stronger H-bond acceptors than water. Owing to its unique H-bonding capability, formamide can exist as both cyclic dimers and linear chain oligomers in liquid phase at room temperature. The structures of formamide in its gas,[13] amorphous,[14] and crystalline[15] phases have also been investigated through experiments,[12–25] simulations,[26] and theoretical calculations.[8,9] Recently, several authors have looked at equilibrium and excited state dynamics of formamide by using nonlinear spectroscopic techniques.[1,2] All these activities are partially motivated by the fact that formamide can be used as a model system for studying the hydrogen bonding interactions that occur between amido protons on a hydrated protein backbone. Since formamide contains important structural units such as carbonyl and amino groups as well as peptide bonds, this molecule stands as the simplest building block for amide based catenane and rotaxane systems that are used as excellent molecular templates for tailoring materials with user-defined properties.[27–30] It is also predicted that the coupling between the low frequency vibrations in formamide may play an important role for conformational changes and enzymatic actions in biological systems.[31,32] For example, an out-of-plane vibrational mode of a hydrogen bonded system is likely to be involved in a conformational change in a biologically relevant moiety.

Ion transport and solvation processes in formamide should therefore be investigated in detail in order to understand the solute-solvent interaction and dynamics in liquid formamide.[33–41] The interesting question that one would like to ask here is that whether a simple theory can describe the diffusion and solvation processes in such an associated solvent where several geometrical isomers are present in its liquid state. We have addressed this aspect in the present article. We would also like to investigate the following question: To what extent can the ultrafast solvent response of subpicosecond time scale control a diffusive process such as ion conductance which takes place on a time scale of tens of picoseconds or even longer?

Any discussion on ionic conductivity starts with Kohlrausch's law which is given as follows:[33–36]

$$\Lambda_m = \Lambda_0 - \kappa\sqrt{c}, \tag{1}$$

where Λ_m represents the equivalent molar conductivity, Λ_0 is its limiting value at infinite dilution, and κ is a coefficient that is found to depend more on the nature of the electrolyte than on its specific identity. Extrapolation of Λ_m to zero ion concentration produces Λ_0. Equation (1) is valid for the conductivity of the electrolyte where the dissociation is complete.

The equivalent conductivity at infinite dilution, Λ_0, is essentially related to the ion mobility U under the influence of externally applied weak electric field in the following manner:[33–35]

$$\Lambda_0 = UF = |q|\frac{F}{\varsigma} = \frac{|q|F}{A\eta_0 r_{\text{ion}}}, \tag{2}$$

where F stands for Faraday constant and q the charge on the ion. ς is the ionic friction coefficient. The third equality in the above equation arises if one assumes that the friction experienced by an ion with crystallographic radius, r_{ion}, moving through a solvent with viscosity, η_0, can be obtained from hydrodynamics by using Stokes'law. The value of A

a)Author to whom correspondence should be addressed. Electronic mail: ranjit@bose.res.in

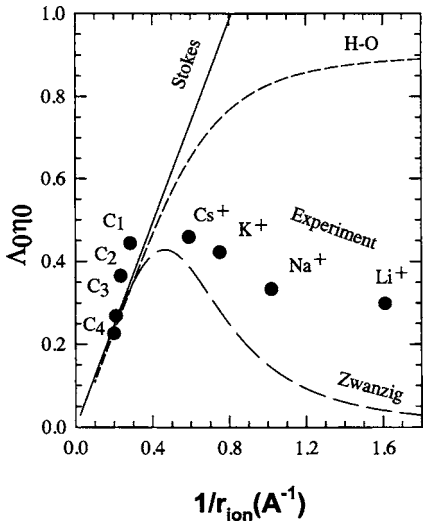

FIG. 1. Comparison between the experimental results (solid circles) of Walden product ($\Lambda_0\eta_0$) for the unipositive alkali, and tetra-alkyl ammonium ions as a function of inverse of crystallographic radius (r_{ion}^{-1}) for formamide at room temperature with the predicted values of Stokes's law (solid line), Hubbard-Onsager theory (short dashed line), and continuum theory of Zwanzig (long dashed line). Here, the tetra-alkyl ammonium ions are represented by C_1-C_4 where $C_n=(C_nH_{2n+1})_4N^+$; n is from 1 to 4. The experimental data shown here are taken from Ref. 72.

could be 4π or 6π depending upon boundary condition (slip or stick). This immediately tells us that $\Lambda_0\eta_0$ is proportional to the inverse of the crystallographic radii of the ions in a given solvent. This is known as *Walden's rule* and was found to be valid for large singly charged ions.[33–36] However, as the ions become smaller, the deviation becomes larger leading to a stronger nonmonotonic ion size dependence. This is shown in Fig. 1.

Initially, the breakdown of Walden's rule was explained in terms of *solvent-berg* model[33,34] which proposes that the solvent molecules in the immediate vicinity of the ion stick to it, thereby making a composite body. The effective size of such composite unit increases in size as ion becomes smaller. However, this model fails severely to explain the limiting ionic conductivity of small rigid ions, such as unipositive alkali metal ions.

Later, Born suggested that in addition to the mechanical (bare) friction, the ion experiences a retardation due to the coupling of its electric field with solvent polarization while moving through the solvent. So, the total friction on the ion is expressed as follows:[42]

$$\varsigma_{total} = \varsigma_{bare} - \varsigma_{df}, \tag{3}$$

where the bare friction $\varsigma_{bare}=A\eta_0 r_{ion}$ and ς_{df} is termed as dielectric friction. Fuoss, Boyd, and Zwanzig further developed the dielectric friction model.[43–45] The prediction of Zwanzig's theory[45] for ions in formamide is shown in Fig. 1. In all these models, the solvent was treated as a structureless continuum characterized by frequency dependent dielectric function and a single Debye relaxation time, τ_D.

Hubbard and Onsager studied the ion mobility within the framework of continuum picture[46] and their self-consistent theoretical approach led to the following expression for total friction:[47,48]

$$\frac{1}{\varsigma_{total}} = \int_{r_{ion}}^{\infty} \frac{dr}{4\pi r^2 \eta(r)}, \tag{4}$$

where r is the distance from the surface of the ion. $\eta(r)$ is the distance dependent viscosity given as[47] $\eta(r)=\eta_0[1+\tau_D q^2(\varepsilon_0-\varepsilon_\infty)/16\pi\eta_0\varepsilon_0^2 r^4]$ where η_0 is the zero frequency shear viscosity of the solvent and ε_0 and ε_∞ denote the static and infinite frequency dielectric constants, respectively. The prediction from the H–O theory, shown in Fig. 1, indicates that this theory is also inadequate for describing the experimental limiting ionic conductivities of small ions in formamide. It was later shown empirically that the limiting ionic conductivity could be partially controlled by the solvent diffusion that is related to a variety of molecular motions as well as coupling between them.[49]

Subsequently, Wolynes and co-worker[50–52] developed a theory that took into account the ion-solvent interactions, microscopic solvent structure around an ion to describe the ion conductivity. However, this theory also neither included the full dynamics of the liquid nor the effects of the self-motion of the ion and therefore enjoyed a limited success.

Recently, a generalized molecular theory that incorporates the complex dynamics of polar solvents as well as the self-motion of the ion has been developed by Bagchi and co-workers.[40,53–57] This theory has been found to predict successfully the experimental results in water, D_2O, acetonitrile, and alcohols. We have used this theory to calculate the Λ_0 in formamide. It is to be noted here that the above theory predicts a dynamic cooperativity of solvent translational modes that affects the conductivity in a nonlinear way.[40]

Computer simulation studies for ion conductance in neat amide solvents have not been performed so far, even though ion transport in some other solvent systems has been simulated.[58–60] The complex nature of the solvent and non-availability of proper model potential might be the reasons for this. However, Puhovski and Rode studied the limiting ionic mobility of small, rigid ions such as Na^+ in aqueous mixture of formamide by using the molecular dynamics simulation[59] method. These authors found in this work that Na^+ is preferentially solvated by formamide molecules which is in agreement with the existing NMR data.

The motivation for studying the ion transport and solvation dynamics in formamide comes further from the following facts. First, experimental results for both limiting ionic conductivity and solvation dynamics (dipolar) in liquid formamide at room temperature are available. Second, one would like to explore the effects of the intermolecular vibration (liberation) bands in the range of 100–200 cm^{-1} that have been observed repeatedly in the low frequency Raman studies of amide systems. One wonders here whether this low frequency motion could contribute to the initial fast solvent reorganization and hence makes the solvation energy relaxation ultrafast. This is important as we have observed earlier that inclusion of these bands gives rise to better description of both limiting ionic conductance and solvation dynamics in polar solvents, such as water, D_2O, and *N*-methyl amides.[40,54–57,61,62] However, we are not aware of any experiments that indicate fraction wise contribution of these bands (one at ~110 cm^{-1} and another at ~200 cm^{-1})

to the dielectric dispersion from ε_∞ to the square of the refractive index in liquid formamide. Therefore, we have assumed that the band at 110 cm^{-1} is responsible for the missing part as indicated above. We have performed calculations both with and without this band and presented results in this article. Third, the total limiting ionic conductance (Λ_{total}) in formamide shows interesting temperature dependence. In the above molecular theory, the temperature dependence enters through the generalized rate of solvent polarization relaxation (via the frequency dependent dielectric relaxation data), and solute-solvent and solvent-solvent static correlation functions. One would therefore like to see whether the above molecular theory could explain the observed temperature dependence of Λ_{total} in formamide.

As already mentioned, solvation dynamics is intimately related to the ion transport processes and hence study of solvation dynamics is crucially important for understanding the microscopic mechanism of ion conductance. For example, consider the motion of Li^+ in a solvent with $\tau_D \sim 40$ ps. By using the experimental value of Λ_0 for Li^+ in formamide in the following expression, $D=\Lambda_0(k_BT/q^2N_A)$, one obtains the diffusion coefficient of Li^+ as $\sim 2.4 \times 10^{-6}$ cm^2 s^{-1}. This, after inserting into the Einstein relation, produces $\langle l^2\rangle^{1/2}=\sqrt{6D\tau_D}=0.24$ nm. This is the diffusion displacement of lithium ion over a time period of 40 ps. However, the displacement of this ion with mobility $U=9.4\times 10^{-5}$ cm^2 V^{-1} s^{-1} in the direction of the applied field $E=1$ V cm^{-1} is $l_E=UE\tau_D=3.8\times 10^{-8}$ nm at typical experimental conditions. Interestingly, this value is seven orders less in magnitude than the calculated value of $\langle l^2\rangle^{1/2}$. This means that the motion of the ion between the electrodes is very irregular and the limiting ionic conductivity is determined by random collisions of the moving ion with the solvent environment and thus both by structure and dynamics.[59,60]

The organization of the rest of the paper is as follows. Section II contains the theoretical formulation. The method of calculation is discussed briefly in Sec. III. Numerical results are presented in Sec. IV. The article ends with a discussion in Sec. V.

II. THEORETICAL FORMULATION

This section starts with the well-known Kirkwood formula[63] for dielectric friction, ς_{df}, as

$$\varsigma_{df}=\frac{1}{3k_BT}\int dt\langle \mathbf{F}_{id}(0)\cdot\mathbf{F}_{id}(t)\rangle, \tag{5}$$

where $\mathbf{F}_{id}(t)$ is the time dependent force acting on the ion due to ion-dipole interaction and k_BT is Boltzmann's constant times temperature. $\mathbf{F}_{id}(t)$, which is responsible for the dielectric friction, is long range in nature. The density functional theory (DFT) is used to obtain the following expression for the force density on the ion due to ion-dipole interaction as[40,41]

$$\mathbf{F}_{id}(\mathbf{r},t)=k_BT\mathbf{n}_{ion}(\mathbf{r},t)\,\nabla\int d\mathbf{r}'d\mathbf{\Omega}'c_{id}(\mathbf{r};\mathbf{r}',\mathbf{\Omega}') \times\delta\rho(\mathbf{r}',\mathbf{\Omega}',t), \tag{6}$$

where $\mathbf{n}_{ion}(\mathbf{r},t)$ is the number density of ion; $\delta\rho(\mathbf{r},\mathbf{\Omega},t)=\rho(\mathbf{r},\mathbf{\Omega},t)-\rho_0/4\pi$ is the space (r), orientation ($\mathbf{\Omega}$), and time (t) dependent fluctuation in the number density ρ_0 of the pure solvent; and $c_{id}(\mathbf{r};\mathbf{r}',\mathbf{\Omega})$ is the space and orientation dependent ion-dipole direct correlation function (DCF). Now, the space, orientation, and time dependent number density of the solvent and space and orientation dependent DCF are expanded in spherical harmonics. The standard Gaussian decoupling approximation is then used to obtain the following expression for frequency dependent dielectric friction:[40,54–57]

$$\varsigma_{df}(z)=\frac{2k_BT\rho_0}{3(2\pi)^2}\int dte^{-zt}\int dkk^4S_{ion}(k,t) \times c_{id}^{10}(k)^2S_{solvent}^{10}(k,t). \tag{7}$$

where $c_{id}^{10}(k)$ and $S_{solvent}^{10}(k,t)$ are the longitudinal component of ion-dipole DCF and orientation dynamic structure factor of the pure solvent, respectively. In the definition of the above correlation function the wave vector $\boldsymbol{k}$ is taken parallel to the z axis of laboratory fixed frame. $S_{ion}(k,t)$ denotes the self-dynamic structure factor of the ion. In Eq. (7) the self-dynamic structure factor of the ion is assumed to be given by[40]

$$S_{ion}(k,t)=\exp[-D_T^{ion}k^2t]=\exp\left[-\left(\frac{k_BT}{\varsigma_{bare}+\varsigma_{df}}\right)k^2t\right], \tag{8}$$

where the diffusion coefficient of the ion, D_T^{ion}, itself depends on the total friction.

The orientational dynamic structure factor of the pure solvent is calculated by using the following expression:[40]

$$S_{solvent}^{10}(k,t)=\frac{1}{4\pi 3Y}\left[1-\frac{1}{\varepsilon_L(k)}\right]L^{-1}\left[\frac{1}{z+\Sigma_{10}(k,z)}\right], \tag{9}$$

where L^{-1} stands for Laplace inversion. $3Y$ is the polarity parameter of the solvent which is related to the dipole-moment μ and density ρ_0 of the solvent by the relation $3Y=(4\pi/3k_BT)\mu^2\rho_0$. $\varepsilon_L(k)$ is the longitudinal component of wave number dependent dielectric function. $\Sigma_{10}(k,z)$ is the longitudinal ($l=1$, $m=0$) component of the generalized rate of orientational polarization density relaxation of the solvent and is given by[40,41]

$$\Sigma_{lm}(k,z)=\left[1-\frac{\rho_0}{4\pi}c(llm;k)\right]\left\{\frac{l(l+1)k_BT}{I[z+\Gamma_R(k,z)]} + \frac{k^2k_BT}{m\sigma^2[z+\Gamma_T(k,z)]}\right\}, \tag{10}$$

where m, σ, and I are the mass, diameter, and the average moment of inertia of each solvent molecules, respectively. $c(110,k)$ is the (110) component of the wave number (k) dependent two particle direct correlation function of pure solvent. $\Gamma_R(k,z)$ and $\Gamma_T(k,z)$ are the wave number and frequency (z) dependent rotational the translational dissipative kernels, respectively, of the solvent.

In the $z=0$ limit, Eq. (7) provides the following expression for macroscopic dielectric friction [that is $\varsigma_{df}(z=0) \equiv \varsigma_{df}$]:[40,54–57]

$$\varsigma_{df} = \frac{2k_B T\rho_0}{3(2\pi)^2}\frac{1}{4\pi 3Y}\int_0^\infty dk k^4 |c_{id}^{10}(k)|^2\left[1-\frac{1}{\varepsilon_L(k)}\right] \times \frac{1}{D_T^{ion}k^2 + \Sigma_{10}(k, D_T^{ion}k^2)}. \quad (11)$$

Since the diffusion coefficient of the ion, D_T^{ion}, itself depends on the total friction, Eq. (11) must be solved self-consistently. Once ς_{df} is calculated self-consistently, Eq. (3) is used to obtain the total friction experienced by the ion where the bare friction (ς_{bare}) is calculated from Stokes' law by using the slip boundary condition. The limiting ionic conductivity at infinite dilution is then obtained by using the relation $\Lambda_0=[qF]^2/RT\varsigma_{total}$, where R is the Avogadro number times the Boltzmann constant.

One can again use the density functional theory to obtain the expression for the time dependent solvation energy for a mobile dipolar solute. It has already been observed that the self-motion (both rotational and translational) of the dipolar solute can contribute to the solvation dynamics by offering an extra channel to the energy relaxation process.[64] One can find a rigorous derivation of relevant expressions in Ref. 64. However, the probe molecules that are frequently used in solvation dynamics experiments are often massive and contain several aromatic rings and therefore several times bigger than a solvent molecule. This means that the probe solute remains practically immobile during the course of solvation and therefore the solvation becomes that of an immobile solute. In such a scenario the expression for the time dependent solvation energy for a dipolar solute can be given as follows:[40,64]

$$E_{sol}(\mathbf{r},\mathbf{\Omega},t) = -k_B T\int d\mathbf{r}' d\mathbf{\Omega}' c_{sd}(\mathbf{r},\mathbf{\Omega};\mathbf{r}',\mathbf{\Omega}') \times \delta\rho(\mathbf{r}',\mathbf{\Omega}',t), \quad (12)$$

where $E_{sol}(\mathbf{r},\mathbf{\Omega},t)$ is the solvation energy of a immobile dipolar solute located at position $\mathbf{r}$ with orientation $\mathbf{\Omega}$ at a time t. $c_{sd}(\mathbf{r},\mathbf{\Omega};\mathbf{r}',\mathbf{\Omega}')$ denotes the direct correlation function between the solute dipole and a solvent dipole at positions $\mathbf{r}$ and $\mathbf{r}'$ with orientations $\mathbf{\Omega}$ and $\mathbf{\Omega}'$, respectively. The direct correlation function c_{sd} contains detailed microscopic information about the orientational structure of solution. The density of the solute dipole is assumed to be very small so that the interaction among them can be neglected. Then, a straightforward algebra leads to the following expression for the normalized solvation energy autocorrelation function:[64]

$$S(t) = \frac{\int_0^\infty dk k^2\left\{|c_{sd}^{10}(k)|^2\left[1-\frac{1}{\varepsilon_L(k)}\right]L^{-1}[z+\Sigma_{10}(k,z)]^{-1} + 2|c_{sd}^{11}(k)|^2[\varepsilon_T(k)-1]L^{-1}[z+\Sigma_{11}(k,z)]^{-1}\right\}}{\int_0^\infty dk k^2\left\{|c_{sd}^{10}(k)|^2\left[1-\frac{1}{\varepsilon_L(k)}\right] + 2|c_{sd}^{11}(k)|^2[\varepsilon_T(k)-1]\right\}}, \quad (13)$$

where $c_{sd}^{10}(k)$ and $c_{sd}^{11}(k)$ are the longitudinal and transverse components of the wave number dependent dipole-dipole direct correlation function and has been calculated using mean spherical approximation (MSA). $\varepsilon_L(k)$ and $\varepsilon_T(k)$ are the longitudinal and transverse components of wave number dependent dielectric constant. $\Sigma_{11}(k,z)$ is the transverse ($l=1$, $m=1$) components of the wave number and frequency dependent generalized rate of solvent orientational polarization density relaxation ($\Sigma_{lm}(k,z)$). This is already defined and given as Eq. (10).

We have used Eq. (13) to calculate the decay of the normalized solvation energy autocorrelation function, $S(t)$, of a dipolar probe coumarin 153 in formamide at 283.15, 298.15, and 328.15 K.

III. CALCULATIONAL PROCEDURE

A. Calculation of the wave number and frequency dependent generalized rate of solvent polarization relaxation, $\Sigma_{lm}(k,z)$

The calculation of the generalized rate of solvent orientational polarization density relaxation, $\Sigma_{lm}(k,z)$, is non-trivial and somewhat involved. The detailed derivation of this quantity has already been presented elsewhere[40,61] and hence we will *briefly* describe the calculation procedure here. It is already mentioned that $\Sigma_{lm}(k,z)$ contains two dissipative kernels—the rotational kernel ($\Gamma_R(k,z)$) and the translational kernel ($\Gamma_T(k,z)$). The rotational kernel is obtained directly from the experimentally measured frequency dependent dielectric function $\varepsilon(z)$ in the following stepwise manner. First, one uses the molecular hydrodynamic theory to relate the wave number dependent memory function exactly to the relevant dynamical correlation function.[61] In the long wavelength (that means $k\to 0$) limit, this reduces to the dielectric relaxation function. Therefore, the k dependence of the rotational memory kernel is neglected and $\Gamma_R(k,z)$ is replaced by $\Gamma_R(k=0,z)$. This approximation has been found to be valid for limiting ionic conductivity and polar solvation dynamics since in both cases the orientational polarization density relaxation is dictated by the long wavelength polarization density fluctuations.[40] Second, $\Gamma_R(k=0,z)$ is related to the experimentally determined frequency dependent dielectric function, $\varepsilon(z)$. The relevant expression and procedure have been described in Refs. 40 and 61.

TABLE I. Dielectric relaxation parameters for formamide at different temperatures.

Temperature (K)	ε_1	τ_1 (ps)	β_1 (DC)[a]	ε_2[b]	n_D[c]	n_D^2
288.15	113.42	55.6	0.91	5.62	1.447	2.094
298.15	109.56	40.3	0.94	5.71	1.447	2.094
328.15	98.75	22.1	0.94	4.80	1.447	2.094

[a]Davidson-Cole (DC) relaxation.
[b]The dispersion $(\varepsilon_2 - n_D^2)$ is assumed to carry out by the librational band at 110 cm^{-1} at all the three temperatures mentioned above.
[c]n_D represents the refractive index.

The experimental data for the frequency dependent dielectric function of formamide at three different temperatures are described by the following rather general expression:[65]

$$\varepsilon(z) = \varepsilon_\infty + \sum_{i=1}^{m} \frac{(\varepsilon_i - \varepsilon_{i+1})}{[1 + (z\tau_i)^{1-\alpha_i}]^{\beta_i}}, \tag{14}$$

where z is Laplace frequency, ε_1 is the static dielectric constant, $\varepsilon_{m+1} = \varepsilon_\infty$ is its limiting value at high frequency, ε_i are intermediate steps in the dielectric constant, m is the number of distinct relaxation processes, and τ_i are their relaxation time constants with relaxation parameters $0 \leqslant \alpha_i < 1$ and $0 < \beta_i \leqslant 1$.

For our calculation in formamide, we have used dielectric relaxation data measured by Barthel and *et al.*[66] who recorded the frequency dependent dielectric function in the range of 0.2–89 GHz. The details of the dielectric relaxation data are summarized in Table I. The interesting aspect of these data is that they are best fitted to a single Davidson-Cole (DC) ($\alpha_i = 0$, $\beta_i < 1$) equation at all the three temperatures studied here. It should also be noted that at these temperatures the value of the measured ε_∞ is approximately 5. Therefore, the dispersion, $(\varepsilon_\infty - n_D^2) = (5 - 2.1) \approx 3$ (n_D being the refractive index) is *missing* in these data which may be due to the limited resolution available to these authors. However, we have seen earlier[62] that such missing component can make the solvation energy relaxation faster and hence contribute in an important manner to both the ultrafast polar solvent response and ionic conductivity in formamide. The experimental study of Chang and Castner[1] by using optical Kerr effect (OKE) spectroscopy has revealed that formamide contains librational modes with frequencies centered at ~110 and ~200 cm^{-1}. These findings have also been corroborated by other authors.[3,4] The works of Cho *et al.*[67] and McMorrow and Lotshaw[68] have shown the connection between dynamics measured by OKE and time dependent fluorescence Stokes'shift (TDFSS) measurements. We have assumed that the librational mode at ~110 cm^{-1} takes part in both the polar solvation energy relaxation and limiting ionic conductivity in formamide at all temperatures studied here. This is done by making the above libration band responsible for the dispersion $(\varepsilon_\infty - n_D^2)$. This is purely exploratory in nature and further experiments with a better time resolution can reveal the missed part of the full relaxation. All the other parameters remained the same. In addition, we have assumed that this librational mode is an overdamped one.

The translational dissipative kernel has been calculated by using the isotropic dynamic structure factor of the liquid. The details regarding the calculation of $\Gamma_T(k,z)$ have been described in Refs. 40 and 55.

B. Calculation of correlation functions

1. Solvent dipole-dipole direct correlation functions, $c(110,k)$ and $c(111,k)$

The solvent orientational, static correlation function, $c(110,k)$ is calculated by using the MSA model for a pure solvent.[69] Then proper corrections at both $k \to 0$ and $k \to \infty$ limits are used to obtain the wave number dependent dielectric function $\varepsilon_L(k)$. Subsequently, the longitudinal component of the wave number dependent dielectric function, $\varepsilon_L(k)$, is obtained by the following exact relation:[40,41]

$$\left[1 - \frac{1}{\varepsilon_L(k)}\right] = \frac{3Y}{1 - (\rho_0/4\pi)c(110,k)}. \tag{15}$$

For intermediate wave numbers ($k\sigma \to 2\pi$), we have used Eq. (15) while for $k \to \infty$ we have used a Gaussian function which begins at the second peak height of $[1\text{-}1/\varepsilon_L(k)]$ to describe the behavior at large k. As described earlier, this procedure removes the wrong wave number behavior of static correlations described by the MSA.

We have obtained the transverse component of the solvent dipole-dipole direct correlation function $c(111,k)$ directly from the MSA. Then the transverse component of wave number dependent dielectric function $\varepsilon_T(k)$ is obtained by using the following relation:[40,41]

$$[\varepsilon_T(k) - 1] = \frac{3Y}{1 + (\rho_0/4\pi)c(111,k)}.$$

2. Ion-dipole direct correlation function, $c_{id}(k)$

The ion-dipole DCF, $c_{id}(k)$, is calculated using the procedure of Chan *et al.*[70] for electrolyte solution in the limit of zero ion concentration. The ions are modeled here as hard spheres with point charges at the centers and the solvent molecules as hard spheres with embedded point dipoles. In addition, the ions are of the same size but different from that of a dipolar solvent particle. The present work also treats the ion-solvent system in the same manner. We first calculate the solvent microscopic polarization $P_{mic}(r)$ around an ion using Eqs. (3.72) and (3.73) given in Ref. 70. Once the $P_{mic}(r)$ is calculated, we use Eqs. (3.67), (3.57), and (3.15b) of the same reference to obtain the ion-dipole direct correlation function $c_{id}(k)$. The behavior of the microscopic polarization,

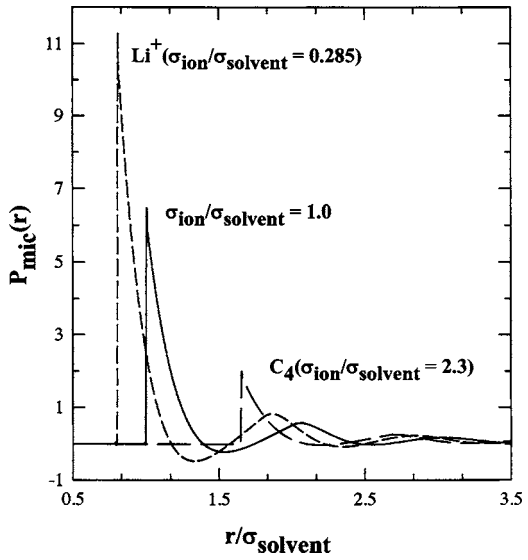

FIG. 2. The microscopic polarization $P_{\mathrm{mic}}(r)$ (scaled by $\sqrt{k_B T/\sigma^3_{\mathrm{solvent}}}$) of solvent around an ion as a function distance r (scaled by solvent diameter $\sigma_{\mathrm{solvent}}$) from the center of the ion. Note the difference in polarization for different ion-solvent (formamide) size ratios. A small negative value of $P_{\mathrm{mic}}(r)$ is also seen which may mean that formamide molecules just outside the first salvation shell are oriented in a direction opposite to those inside the shell. According to the discussion in Ref. 70, this may also be an artifact of the MSA.

$P_{\mathrm{mic}}(r)$, around different ions in formamide has been shown in Fig. 2. Note the difference in $P_{\mathrm{mic}}(r)$ value for ions with different sizes.

We would like to mention here that since the MSA is a linear theory, any modification in the solvent structure around an ion through nonlinear interactions in a solvent of high dielectric constant and dipole moment will be completely missed. Therefore, as correctly pointed out in Ref. 70, the calculated polarization structure around an ion in formamide, as shown in Fig. 2, may not be quantitatively accurate. However, the calculation of ion-dipole direct correlation functions by using the MSA may still be justified because the predictions are semiquantitative in nature with correct trends. Furthermore, no other theory that describes the ion-dipole system better and at simpler level than this are available to us.

3. Solute dipole-solvent dipole direct correlation function, $c_{\mathrm{sd}}(k)$

The value of $c_{\mathrm{sd}}(k)$ is calculated by using the MSA model for a binary mixture of dipolar liquids.[71] Here we have assumed that the formamide is host solvent in which the dipolar probe solute (coumarin 153) is present in the limit of zero concentration. The parameters necessary for obtaining these static correlations have been given in Table II.

IV. NUMERICAL RESULTS AND COMPARISON WITH EXPERIMENTS

This section is divided into two subsections. In the first one we present the calculated limiting ionic conductivities in formamide at different temperatures. A comparison between the theoretical results and experimental data[72] is also shown here. The theoretical predictions for dipolar solvation dynamics of formamide at three different temperatures are presented in the next subsection. The calculated decay of the normalized solvation energy autocorrelation function at 298.15 K is also compared with the available experimental data[38] in this subsection.

TABLE II. Solvent parameters needed for the theoretical calculation at different temperatures.

Temperature (K)	Diameter (A^0)	μ (D)	Density (g/cm^3)	Viscosity (cp)
283.15	4.36	3.72[a]	1.1508	5.00
298.15	4.36	3.72	1.1296	3.31
328.15	4.36	3.72[a]	1.1296 (298.15 K)	1.833 (325.15 K)

[a]The values of μ at temperatures of 283.15 and 328.15 K are not available and hence the value of μ at 298.15 K is used for calculations at the other two temperatures. The values in the parentheses in the "Density" and "Viscosity" columns indicate the temperatures at which these properties were measured.

A. Limiting ionic conductivity and temperature dependence

In Fig. 3 we show the calculated value of the Walden product, $\Lambda_0 \eta_0$, plotted against the inverse of the crystallographic radius of the ion, r_{ion}^{-1}, in formamide at room temperature. The thick solid line represents the predictions from the present theory. For comparison, available experimental data[72] (solid circles) are shown in the same figure. It is clear that the theory agrees well with the experiments. However, the predicted peak position of the Walden product with respect to r_{ion}^{-1} is slightly shifted towards the smaller ions. Figure 3 also shows the calculated values of the Walden product for unipositive ions in formamide predicted by the con-

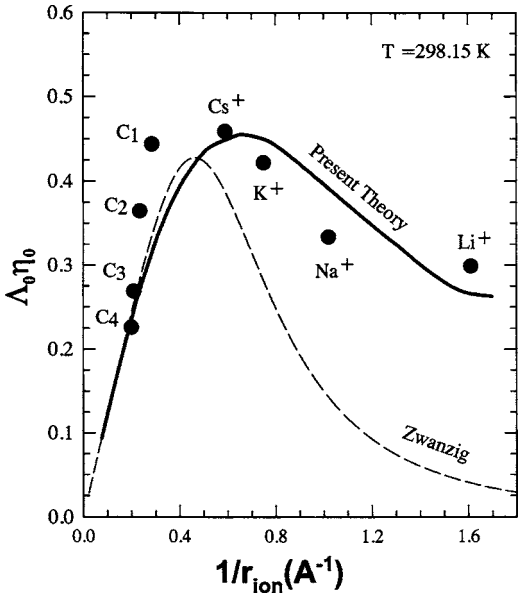

FIG. 3. The limiting values of Walden product $(\Lambda_0 \eta_0)$ for the alkali, and tetra-alkyl ammonium ion as a function of inverse of crystallographic radius (r_{ion}^{-1}) in formamide at room temperature. The solid line represents the prediction of the present microscopic theory, the solid circles denote the experimental results, and the short dashed line represents Zwanzig theory.

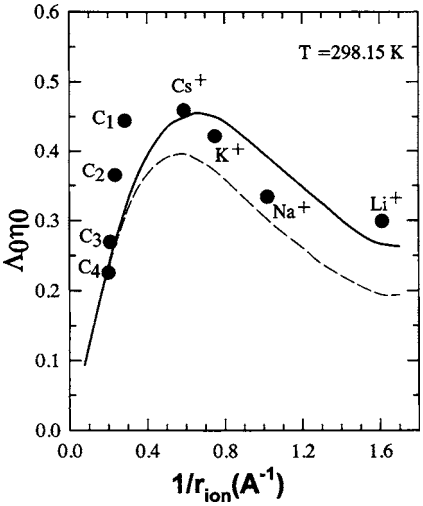

FIG. 4. The effect of libration band (110 cm^{-1}) on the limiting ionic conductivity in formamide at room temperature. The values of Walden product $\Lambda_0\eta_0$ are plotted as a function of the inverse of crystallographic radius of the ions. The solid line represents the prediction of the present theory that includes the contribution of the libration band at 110 cm^{-1} to the dielectric relaxation of formamide. Experimentally obtained Walden products for different ions are denoted by solid circles. The short dashed line represents the prediction of the present theory without the contribution from the libration band.

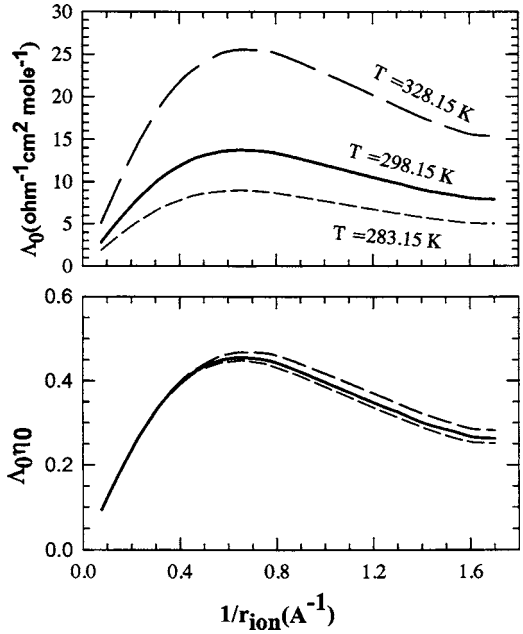

FIG. 5. Upper panel: Temperature dependent limiting ionic conductance Λ_0 for unipositive ions as a function of the inverse of the crystallographic radius (r_{ion}^{-1}). The short dashed line, solid line, and long dashed line represent the predictions of the present molecular theory at 283.15, 298.15, and 328.15 K, respectively. Lower panel: The temperature dependence of the Walden product for the same ions at these three temperatures. The representations remain the same as in the upper panel. For discussion, see text.

tinuum theory of Zwanzig. It is interesting to note that the theory of Zwanzig[45] fails completely for small ions such as Na^+ and Li^+. This is probably due to the neglect of the microscopic structure of the liquid around the moving ion and also not accounting for the fast components of the liquid dynamics that are often exhibited in the recent frequency dependent dielectric relaxation measurements.[66]

The effects of the intermolecular vibration (libration) band with a frequency centered at 110 cm^{-1} on the limiting ionic conductivity are shown in Fig. 4. The solid and dashed lines represent the calculations with and without this band, respectively. As evident from this figure, the agreement between the theory and experiments[72] becomes *poor* if the contribution of this band to the *complete* dielectric relaxation of formamide is neglected. This has been observed *earlier* for water and deuterated water (D_2O) also.[40,54–57,61] As we will see in the next section, this band also contributes *significantly* to the time dependent progress of solvation of a dipolar probe in formamide.

The limiting ionic conductivity, Λ_0, calculated for three different temperatures 283.15, 298.15, and 328.15 K in formamide is shown in the *upper panel* of Fig. 5. The temperature dependent solvent parameters needed for the above calculation are summarized in Table II. Note in the above figure that the calculation predicts a strong temperature dependence of limiting ionic conductivity in formamide. Since the present theory uses the experimentally measured frequency dependent dielectric relaxation data as an input, such a strong temperature dependence originates primarily from the dielectric relaxation parameters obtained at different temperatures. This means that the zero frequency dielectric friction, ς_{df} ($z=0$), is responsible for the observed temperature dependence. We shall come back to this discussion later. We would like to mention here that the calculated values of Λ_0 could not be compared with the experiments at 283.15 and 328.15 K because of the nonavailability of experimental data at these temperatures. Hence these predictions should be tested against experiments. We could, however, compare the total limiting ionic conductivities ($\Lambda_0^T=\Lambda_0^+ + \Lambda_0^-$) of several 1:1 strong electrolytes in this liquid at 283.15 K. Such a comparison is shown in Table III where the ratio between the values of $\Lambda_0^T\eta_0$ obtained at 298.15 and 283.15 K is presented for both experiments and theory (second and third columns, respectively). It is evident from this table that the theory agrees well with the experiments at 283.15 K. We have also

TABLE III. $\Lambda_0^T\eta_0$, the total ionic conductivity at infinite dilution ($\Lambda_0^T=\Lambda_0^+ + \Lambda_0^-$) multiplied with the solvent viscosity (η_0), for 1:1 electrolytes in formamide: temperature dependence.

Salts	Expt. $\Lambda_0^T\eta_0$ (298.15 K)/ $\Lambda_0^T\eta_0$ (283.15 K)	Present theory[a] $\Lambda_0^T\eta_0$ (298.15 K)/ $\Lambda_0^T\eta_0$ (283.15 K)	Present thoery[b] $\Lambda_0^T\eta_0$ (298.15 K)/ $\Lambda_0^T\eta_0$ (328.15 K)
NaCl	1.04	1.02	0.96
KCl	0.98	1.01	0.97
KBr	0.98	1.01	0.97
Me_4NI	0.98	1.01	0.99
Et_4NI	0.98	1.01	0.99
Pr_4NBr	0.99	1.01	0.99
Pr_4NI	0.99	1.01	0.99
Bu_4NBr	1.01	1.01	0.99
Bu_4NI	1.02	1.01	0.99
i-Am_3BuNI	0.99	1.00	0.99

[a]Values for solvent viscosity (η_0) at these temperatures are given in the last column of Table II. For further details, see text.
[b]Theoretical predictions presented in this column could not be compared with experiments due to nonavailability of experimental data at 328.15 K.

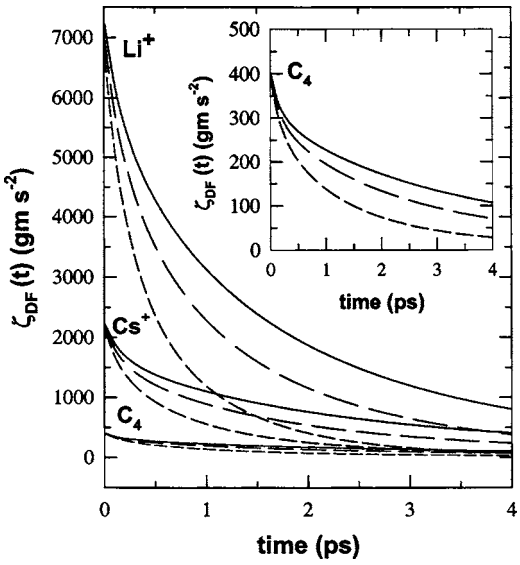

FIG. 6. The time dependent dielectric friction $s_{df}(t)$ experienced by Li^+, Cs^+, and C_4 ions as a function of time t at 283.15 K (solid lines), 298.15 K (long dashed lines), and 328.15 K (short dashed lines). For discussion, see text.

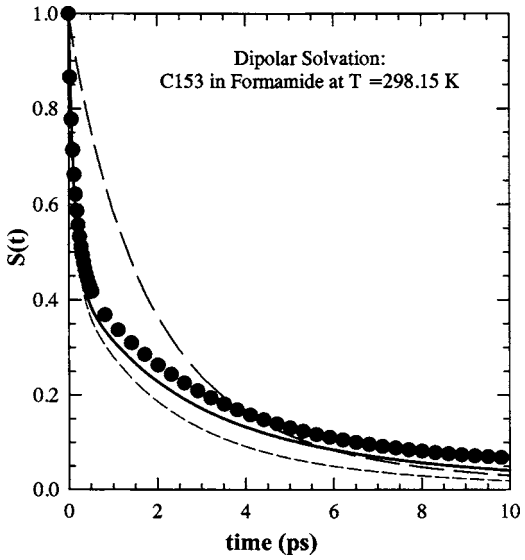

FIG. 7. The normalized solvation energy time autocorrelation function $S(t)$ calculated by using Eq. (13) for a dipolar solute probe (coumarin 153) dissolved in formamide at 298.15 K is shown as a function of time. The theoretical predictions are shown by the solid, short dashed, and long dashed lines and the experiments are by the filled circle. The theoretical prediction represented by the long dashed line is calculated by using the experimental dielectric relaxation data supplied in Ref. 66. The short dashed line is obtained by adding the contribution of the libration band at 110 cm^{-1} band to this dielectric relaxation data. The solid line is obtained by considering the contribution of the libration band and also freezing the translation motion of solvent molecules. Note that the agreement with experiments (solid circles) becomes better upon freezing the solvent translational motion. For further details, see text.

calculated $\Lambda_0^T \eta_0$ at 328.15 K for the same set of electrolytes. The predicted ratios between the values calculated at 298.15 and 328.15 K are shown in the last column of this table. It would be interesting to see if this could also be tested against experiments.

Since viscosity also depends upon temperature, it would be interesting to see how the Walden product for these unipositive ions varies with temperature in formamide. The lower panel of Fig. 5 shows the variation of the Walden product with temperature for these ions. Note here that the temperature dependence in viscosity *offsets* the strong temperature dependence exhibited by the limiting ionic conductivity shown in the upper panel and hence the Walden product becomes almost *insensitive* to the change in temperature.

We now come back to the discussion on the temperature dependence of dielectric friction. The time dependent dielectric friction experienced by Li^+, Cs^+, and C_4 ions while diffusing through formamide at 283.15, 298.15, and 328.15 K is shown in Fig. 6. For clarity, the dependence for the largest ion C_4 is also shown in the *inset*. As expected, the value for the time dependent dielectric friction at the zero time for the smallest on Li^+ is largest while that for the largest ion C_4 is smallest. Also, note that the rate of the decay of time dependent dielectric friction becomes slower as one decreases the temperature.

B. Solvation dynamics and temperature dependence

We now present numerical results of solvation dynamics of an excited dipolar probe solute present at very dilute concentration in liquid formamide at three different temperatures. In our calculation, we have chosen solute parameters as those of coumarin 153 (C153) because we would like to compare the theoretical predictions with the experimental data obtained for the same system by Hong *et al.*[38] We will also present results here to show the effects of the intermolecular vibration band at 110 cm^{-1} on dipolar solvation in formamide. The effect of this band on ionic conductivity is already shown in the previous section.

In Fig. 7 we compare the decay of the normalized solvation energy autocorrelation function, $S(t)$, obtained by using Eq. (13) at 298.15 K with those from the experiments by Hong *et al.*[38] It is evident from this figure that the predicted decay of the normalized solvation energy correlation function (solid line) agrees rather well with the experiments (solid circles). Note here that the numerical results represented by the solid and the short dashed lines are obtained by properly incorporating the contributions from the 110 cm^{-1} band to the complete dielectric relaxation of formamide at 298.15 K. In addition, the solvent molecules are assumed to be *translationally immobile* for the calculated decay represented by the solid line. The long dashed line represents the calculated decay without the 110 cm^{-1} band. It is interesting to note that the experimentally observed short time dynamics is *completely missed* if the contribution from this band is neglected in the present theory. We would also like to mention here that when the solvent molecules are translationally mobile, the decay at long time (>1 ps) predicted by the present theory is faster than what has been observed in experiments. This may be explained as follows. Formamide in the liquid phase can exist as cyclic dimers and linear chain oligomers[1–20] and therefore these large units would be much less mobile (translation) than a single formamide molecule. Consequently, the solvent reorganization around the excited solute (C153) via translational diffusion becomes sluggish

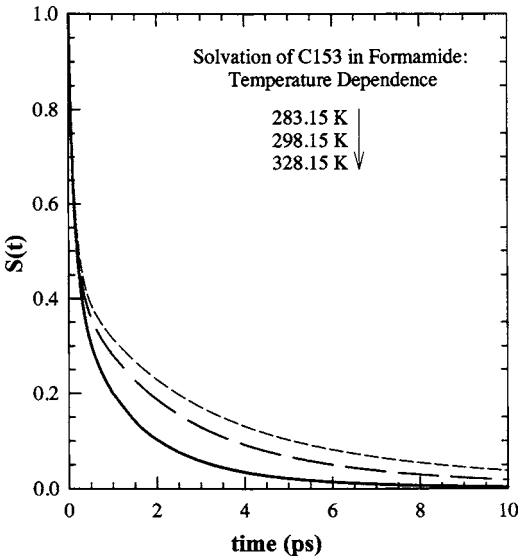

FIG. 8. The effects of temperature on polar solvation energy relaxation in formamide. The normalized solvation energy autocorrelation function $S(t)$ calculated for coumarin 153 in formamide at 283.15 K (short dashed line), 298.15 K (long dashed line), and 328.15 K (solid line) are shown as a function of time (t). Note here that in these calculations, the contributions of the libration band as well as those from the solvent translational mode have been incorporated. In addition, no temperature dependence of the libration band is considered.

and hence the decay rate becomes slower at long time. However, this does not affect the relaxation at short times (<1 ps) because the initial part of the polar solvation energy relaxation is dictated by the intermolecular vibration band (in formamide it is peaked at 110 cm^{-1}) which is *collective* in nature.

In Fig. 8 we present the calculated decay of the solvation energy autocorrelation function $S(t)$ at 283.15 K (solid line), 298.15 K (long dashed line), and 328.15 K (short dashed line). We have assumed here that the librational mode remains peaked at 110 cm^{-1} at all the temperatures studied here. As a consequence of this approximation, at short time the calculated rate of the decay of the normalized solvation energy autocorrelation function becomes the same for these three temperatures. The long time decay, however, becomes slower as the temperature decreases. In all the calculations presented in Fig. 8, the solvent molecules are assumed to be translationally mobile.

V. DISCUSSION

Let us summarize the results presented in this work. We have calculated limiting ionic conductivity of rigid, unipositive ions in formamide at three different temperatures by using a microscopic theory developed earlier. The limiting ionic conductivities predicted by the present theory are found to be in good agreement with the relevant experimental data. The nonmonotonic size dependence of Walden product in formamide has been explained satisfactorily by the present theory as was done earlier for water, deuterated water, acetonitrile, and monohydroxy alcohols.[40,54–57] We have calculated the total limiting ionic conductance of several 1:1 strong electrolytes in formamide at three different temperatures and compared with the available experimental data. We have also studied solvation dynamics of a dipolar solute probe (C153) in formamide in order to investigate the effects of dynamical solvent modes on the ionic mobility in this liquid. A satisfactory agreement between the predicted and experimentally observed decay rates of normalized solvation energy autocorrelation function, $S(t)$, has been found at 298.15 K. Such a comparison for two other temperatures could not be made due to nonavailability of experimental results at these temperatures.

The role of the libration mode centered at 110 cm^{-1} in determining the time scale of the fast component of the polar solvation energy relaxation in formamide and its subsequent effects on ion mobility have also been investigated here. We have found that the fast component of the solvation energy relaxation is totally missed if one switches off the contributions coming from the libration mode. This switching off also overestimates the friction on a moving ion and hence lowers the value of its conductivity at infinite dilution in formamide. We would, however, like to mention here that the coupling of this band to both the solvation dynamics and ionic conductivity through dielectric relaxation is purely an assumption. This assumption together with the results obtained in this article might be regarded as a feedback to the dielectric relaxation studies of liquid formamide. This is because the results indicate that there might be another relaxation step with a time constant present in the subpicosecond regime. Further experiments with more sophisticated technique, such as femtosecond terahertz pulse transmission spectroscopy,[73] may be employed to reveal such a fast time scale in the dielectric relaxation of formamide at the temperatures studied here. Another important aspect of this article is the study of temperature dependence of the Walden product and to use a MSA approach for ion-dipole mixture, which is simple and tractable.

One would now like to ask the following question: why is a simple molecular theory such as the present one successful in predicting the experimentally observed limiting ionic conductivities and polar solvation energy relaxation in a complex liquid like formamide? The following could be the reasons for this success. First, it has already been mentioned earlier that the polar solvation energy relaxation is dominated primarily by the long wavelength ($k\sigma \to 0$) polarization mode and hence contributions from finite wave number processes are either small or negligible. Second, the present theory uses the experimentally measured dielectric relaxation data as an input to calculate the generalized rate of the solvent orientational polarization density relaxation. We believe that the use of the experimentally measured dielectric relaxation data takes care, at least *partially*, of the complex interactions that are present in the solvent. Third, the present theory accounts for the microscopic structure of the solvent and includes the microscopic polarization around a solute ion in a consistent manner.

However, we would like to mention here that in our calculation of dielectric friction, we have neglected the cross correlation between forces arising out of short-range (*hard*) and long-range (*soft*) interactions. This might be erroneous since recent simulation studies by Kumar and Maroncelli[74] have revealed the nonseparability of frictions arising out of

these interactions. This could be a potential source of fatal error and calculations using such scheme may not reflect the correct picture. Their simulation results also demonstrate that whenever the long-range interactions are large enough to significantly affect the friction, the frictional contribution due to the cross correlation between the short-range and long-range forces is of the same magnitude as the friction coming solely from the long-ranged interactions. One therefore needs to develop a theory that will account for the cross correlations in some consistent manner and yet will remain analytically simple such as the present one. This is definitely a challenging task.

ACKNOWLEDGMENTS

We thank Professor Biman Bagchi for several discussions and encouragement. Financial assistances from the University Grants Commission, India and the Council of Industrial and Scientific Research are also gratefully acknowledged.

[1] Y. J. Chang and E. W. Castner, Jr., J. Chem. Phys. **99**, 113 (1993).
[2] J. Park, J. H. Ha, and M. Hochstrasser, J. Chem. Phys. **121**, 7281 (2004).
[3] K. Goossens, L. Smeller, and K. Heremans, J. Chem. Phys. **99**, 5736 (1993).
[4] O. F. Nielsen, P. A. Lund, and E. Praestgaard, J. Chem. Phys. **77**, 3878 (1982).
[5] A. Engdahl, B. Nelander, and P. Astrand, J. Chem. Phys. **99**, 4894 (1993).
[6] R. Ludwig, F. Weinhold, and T. C. Farrar, J. Chem. Phys. **103**, 3636 (1995).
[7] S. Chalmet and M. F. R. Lopez, J. Chem. Phys. **111**, 1117 (1999).
[8] E. Tsuchida, J. Chem. Phys. **121**, 4740 (2004).
[9] D. H. A. ter Steege, C. Lagrost, W. J. Buma, D. A. Leigh, and F. Zerbetto, J. Chem. Phys. **117**, 8270 (2002).
[10] M. Oguni and C. A. Angell, J. Chem. Phys. **78**, 7334 (1983).
[11] A. Mortensen, O. F. Nielsen, J. Yarwood, and V. Shelley, J. Phys. Chem. **98**, 5221 (1994).
[12] R. Ludwig, J. Bohmann, and T. C. Farrar, J. Phys. Chem. **99**, 9681 (1995).
[13] R. J. Kurland and E. B. Wilson, J. Chem. Phys. **27**, 585 (1957); C. C. Costain and J. M. Dowling, *ibid.* **32**, 158 (1960).
[14] S. Nasr and L. Bosio, J. Chem. Phys. **108**, 2297 (1998).
[15] J. Ladell and B. Post, Acta Crystallogr. **7**, 559 (1954).
[16] R. J. de Sando and G. H. Brown, J. Phys. Chem. **72**, 1088 (1968).
[17] E. D. Stevens, Acta Crystallogr., Sect. B: Struct. Crystallogr. Cryst. Chem. **B34**, 544 (1978).
[18] F. J. Weismann, M. D. Zeidler, H. Bartognolli, and P. Chieux, Mol. Phys. **57**, 345 (1986).
[19] M. Kitano and K. Kuchitsu, Bull. Chem. Soc. Jpn. **47**, 67 (1974).
[20] S. L. Whittenburg, V. K. Jain, and S. J. McKinnon, J. Phys. Chem. **90**, 1004 (1986).
[21] E. Hirota, R. Sugisaki, C. J. Nielsen, and G. O. Sorensen, J. Mol. Spectrosc. **49**, 251 (1974).
[22] J. Barthel, K. Buchner, J. B. Gill, and M. Kleebauer, Chem. Phys. Lett. **167**, 62 (1990).
[23] J. Barthel and K. Buchner, Pure Appl. Chem. **63**, 1473 (1991).
[24] T. Drakenberg and S. Forsen, J. Phys. Chem. **74**, 1 (1970).
[25] M. I. Burgar, T. E. Amour, and D. Fiat, J. Phys. Chem. **55**, 1049 (1981).
[26] K. P. Sagarik and R. Ahlrichs, J. Chem. Phys. **86**, 5117 (1987).
[27] D. A. Leigh, A. Murphy, J. P. Smart, and A. M. Z. Slawin, Angew. Chem., Int. Ed. Engl. **36**, 728 (1997).
[28] D. A. Leigh and A. Murphy, Chem. Ind. **178** (1999).
[29] V. Bermudez, N. Capron, T. Gase, F. G. Gatti, F. Kajzar, D. A. Leigh, F. Zerbetto, and S. Zhang, Nature (London) **406**, 608 (2000).
[30] A. M. Brouwer, C. Frochot, F. G. Gatti, D. A. Leigh, L. Mottier, F. Paolucci, S. Roffia, and G. W. H. Wurpel, Science **291**, 2124 (2001).
[31] O. F. Nielsen, P. A. Lund, and E. Praestgaard, J. Chem. Phys. **75**, 1586 (1981); J. Raman Spectrosc. **9**, 286 (1980).
[32] O. F. Nielsen, P. A. Lund, and S. B. Petersen, J. Am. Chem. Soc. **104**, 1991 (1982).
[33] S. Glasstone, *An Introduction to Electrochemistry* (Litton Education, New York, 1942); J. O'M Bockris and A. K. N. Reddy, *Modern Electrochemistry* (Plenum, New York, 1973); P. W. Atkins, *Physical Chemistry*, 5th ed. (Oxford University Press, Oxford, 1994), Pt. III, Chap. 24.
[34] H. S. Harned and B. B. Owen, *The Physical Chemistry of Electrolyte Solutions*, 3rd ed. (Reinhold, New York, 1958).
[35] H. S. Frank, *Chemical Physics of Ionic Solutions* (Wiley, New York, 1956); R. A. Robinson and R. H. Stokes, *Electrolyte Solutions* (Butterworth, London, 1959); R. L. Kay, in *Water: A Comprehensive Treatise*, edited by F. Franks (Plenum, New York, 1973), Vol. 3.
[36] R. L. Kay and D. F. Evans, J. Phys. Chem. **70**, 2325 (1966).
[37] R. Jimenez, G. R. Fleming, P. V. Kumar, and M. Maroncelli, Nature (London) **369**, 471 (1994); M. Maroncelli, J. McInnis, and G. R. Fleming, Science **243**, 1674 (1989).
[38] M. L. Horng, J. A. Gardecki, A. Papazyan, and M. Maroncelli, J. Phys. Chem. **99**, 17311 (1995).
[39] D. Bingemann and N. P. Ernsting, J. Chem. Phys. **102**, 2691 (1995); N. P. Ernsting, N. E. Konig, K. Kemeter, S. Kovalenko, and J. Ruthmann, AIP Conf. Proc. **441**, (1995); B. M. Ladanyi and R. M. Stratt, J. Phys. Chem. **100**, 1266 (1996).
[40] B. Bagchi and R. Biswas, Adv. Chem. Phys. **109**, 207 (1999) and references therein.
[41] B. Bagchi and A. Chandra, Adv. Chem. Phys. **80**, 1 (1991); B. Bagchi, Annu. Rev. Phys. Chem. **40**, 115 (1989).
[42] M. Born, Z. Phys. **1**, 45 (1920).
[43] R. M. Fuoss, Proc. Natl. Acad. Sci. U.S.A. **45**, 807 (1959).
[44] R. H. Boyd, J. Chem. Phys. **35**, 1281 (1961); **39**, 2376 (1963).
[45] R. Zwanzig, J. Chem. Phys. **38**, 1603 (1963); **52**, 3625 (1970).
[46] J. B. Hubbard and L. Onsager, J. Chem. Phys. **67**, 4850 (1977); J. B. Hubbard, *ibid.* **68**, 1649 (1978).
[47] J. B. Hubbard and P. G. Wolynes, in *The Chemical Physics of Solvation*, edited by R. R. Dogonadze, E. Kalman, A. A. Kornyshev, and J. Ulstrup (Elsevier, New York, 1988), Pt. C, Chap. 1, p. 33.
[48] J. B. Hubbard and R. F. Kayser, J. Chem. Phys. **74**, 3535 (1981); **76**, 3377 (1982).
[49] Y. M. Kessler, R. S. Kumeev, I. I. Vaisman, R. B. Lyalina, and R. H. Bratishko, Ber. Bunsenges. Phys. Chem. **93**, 770 (1989).
[50] P. G. Wolynes, J. Chem. Phys. **68**, 473 (1978).
[51] P. Colonomos and P. G. Wolynes, J. Chem. Phys. **71**, 2644 (1979).
[52] P. G. Wolynes, Annu. Rev. Phys. Chem. **31**, 345 (1980).
[53] B. Bagchi, J. Chem. Phys. **95**, 467 (1991).
[54] R. Biswas, S. Roy, and B. Bagchi, Phys. Rev. Lett. **75**, 1098 (1995).
[55] R. Biswas and B. Bagchi, J. Chem. Phys. **106**, 5587 (1997).
[56] R. Biswas and B. Bagchi, J. Am. Chem. Soc. **119**, 5946 (1997).
[57] B. Bagchi and R. Biswas, Acc. Chem. Res. **31**, 181 (1998).
[58] S. H. Lee and J. C. Rasaiah, J. Chem. Phys. **101**, 6964 (1994); J. Phys. Chem. **100**, 1420 (1996).
[59] Y. P. Puhovski and B. M. Rode, J. Chem. Phys. **107**, 6908 (1997).
[60] Y. P. Puhovski and B. M. Rode, J. Chem. Phys. **102**, 2920 (1995).
[61] S. Roy and B. Bagchi, J. Chem. Phys. **99**, 1310 (1993); N. Nandi, S. Roy, and B. Bagchi, *ibid.* **102**, 1390 (1995).
[62] R. Biswas and B. Bagchi, J. Phys. Chem. **100**, 1238 (1996).
[63] J. G. Kirkwood, J. Chem. Phys. **14**, 180 (1946).
[64] R. Biswas and B. Bagchi, J. Phys. Chem. **100**, 4261 (1996).
[65] See, for example, *Theory of Electric Polarization*, 78th ed., edited by C. J. F. Bottcher and P. Bordewijck (Elsevier, Amsterdam, 1978), Vol. II.
[66] J. Barthel, R. Buchner, and B. Wurm, J. Mol. Liq. **98–99**, 51 (2002).
[67] M. Cho, S. J. Rosenthal, N. F. Scherer, L. D. Ziegler, and G. R. Fleming, J. Chem. Phys. **96**, 5033 (1992).
[68] D. McMorrow and T. Lotshaw, J. Phys. Chem. **95**, 10395 (1991).
[69] C. G. Gray and K. E. Gubbins, *Theory of Molecular Fluids* (Clarendon, Oxford, 1984), Vol. I.
[70] D. Y. C. Chan, D. J. Mitchel, and B. Ninham, J. Chem. Phys. **70**, 2946 (1979).
[71] D. Isbister and R. J. Bearman, Mol. Phys. **28**, 1297 (1974); S. A. Adelman and J. M. Deutch, J. Chem. Phys. **59**, 3971 (1973).
[72] J. Thomas and D. F. Evans, J. Phys. Chem. **74**, 3812 (1970).
[73] J. T. Kindt and C. A. Schmuttenmaer, J. Phys. Chem. **100**, 10373 (1996).
[74] P. V. Kumar and M. Maroncelli, J. Chem. Phys. **112**, 5370 (2000).